Ionization and Reprotonation of Self-Assembled Mercaptopropionic Acid Monolayers Investigated by Surface Plasmon Resonance Measurements

ARTICLE *in* LANGMUIR · JANUARY 2002

Impact Factor: 4.46 · DOI: 10.1021/la011226y

5 AUTHORS, INCLUDING:

Jingang Yi
Rutgers, The State University of New Jersey
125 PUBLICATIONS **1,550** CITATIONS
SEE PROFILE

Chris M. Pettit
Emporia State University
25 PUBLICATIONS **540** CITATIONS
SEE PROFILE

Dipankar Roy
Clarkson University
131 PUBLICATIONS **2,542** CITATIONS
SEE PROFILE

Ionization and Reprotonation of Self-Assembled Mercaptopropionic Acid Monolayers Investigated by Surface Plasmon Resonance Measurements

S. Chah,[†] J. Yi,[†] C. M. Pettit,[‡] D. Roy,*[,‡,§] and J. H. Fendler*[,‡,||]

Center for Advanced Materials Processing and Department of Physics, Clarkson University, Potsdam, New York 13699, and Environmental Materials and Process Laboratory, School of Chemical Engineering, Seoul National University, Seoul 151-742, South Korea

Received August 1, 2001. In Final Form: November 6, 2001

We have investigated self-assembled monolayers (SAMs) of 3-mercaptopropionic acid (MPA) on gold substrates by using angle and time-resolved surface plasmon resonance (SPR) measurements. The angle-resolved SPR measurements, carried out in two solvents (ethanol and water) and at two wavelengths (632.8 and 850.0 nm), lead to a value of 0.50 ± 0.02 nm for the thickness of the MPA SAM. Employing a high-resolution bicell photodetector for time-resolved SPR, we have determined the rate constant for the formation of MPA SAM in water to be 7.54×10^{-3} min^{-1}. By combining the results of the two types of SPR experiments, we determined the change of refractive index ($\sim 10^{-3}$ refractive index units) as a function of MPA ionization and reprotonation.

1. Introduction

Self-assembled monolayers (SAMs) of functionalized alkanethiols on gold substrates are the most often employed templates for the chemical construction of advanced electronic devices and sensors.[1,2] The self-assembly is governed by the formation of strong S−Au bonds and by the hydrophobic interactions between the alkyl chains of the thiols.[3] SAMs formed from long chain (>C-16) alkanethiols provide a defect-free coverage of the surface and mediate charge transfer by electron tunneling between molecules (or clusters or nanoparticles) attached onto their functionalized end and the gold substrate. In contrast, short chain (<C-4) functionalized alkanethiols form loosely packed SAMs which permit the attached charge carriers to transfer electrons directly to (or from) the gold substrate. Mercaptopropionic acid SAMs have been advantageously utilized for attaching proteins,[4] DNA,[5] and a variety of other electron-transfer agents[6] onto substrates. 3-Mercaptopropionic acid (MPA) SAMs have also been employed in the fabrication of nanopores[6,7] (and hence nanopatterned surfaces) as well as for the stabilization of size-selected metallic (i.e., monolayer protected clusters, MPCs)[8] and semiconducting nanoparticles.[9] Understanding and controlling the self-assembly of MPA and of the factors which determine the surface charge and charge density of MPA SAMs is of fundamental importance and practical utility for the design of devices and sensors. As part of our overall interest in surface plasmon resonance (SPR) imaging,[9] we have undertaken a systematic investigation of the factors which influence the formation of SAMs from carboxyl- and amine-functionalized alkanethiols. We report here the first SPR observation of the ionization and reprotonation of a MPA SAM on a gold substrate. Taking advantage of a sensitive SPR instrument using a bicell photodetector, we have readily observed pH-dependent differences in the reflectivity of a MPA SAM on a gold substrate and elucidated the rate of MPA self-assembly. Additionally, by combining two-solvent and two-color angle-dependent SPR measurements, we have determined the thickness of the MPA SAM, and by correlating the results of the angle and time-resolved measurements, we have elucidated the changes in the refractive index of the MPA layer which accompanied ionization and reprotonation.

2. Theoretical Considerations

We utilize a five-phase multilayer SPR system,[10,11] denoted as (01234), in the Kretschmann configuration using attenuated total reflection (ATR).[12,13] A schematic diagram of this system has been presented in one of our recent reports.[14] The different phases in the SPR device are labeled as follows: 0, a glass slide (SF10), optically coupled to a 90° ATR prism of the same material; 1, a thin (≤0.4 nm) binder layer of Cr; 2, a layer (∼40−45 nm) of Au deposited on the Cr film; 3, a carboxylic acid terminated SAM of MPA; 4, an ambient dielectric of pH-controlled water. For certain measurements in this work, we also use ethanol for medium 4. The dielectric function and thickness of the mth layer in the five-phase system are denoted as ϵ_m and d_m, respectively. At a given wavelength (λ) of the probe light, the reflectivity (R) of the multilayer system depends on the incidence angle (θ_0 in medium 0),

* Corresponding authors.
[†] Seoul National University.
[‡] Department of Physics, Clarkson University.
[§] E-mail: samoy@clarkson.edu. Phone: (315) 268-6676. Fax: (315) 268-6610.
[||] E-mail: fendler@clarkson.edu. Phone: (315) 268-7113. Fax: (315) 268-4416.

(1) Ulman, A. *Chem. Rev.* **1996**, *96*, 1533.
(2) Fendler, J. H. *Chem. Mater.* **2001**, *31*, 3196.
(3) Fendler, J. H. *Chem. Mater.* **1996**, *8*, 1616.
(4) Li, J. H.; Cheng, G. J.; Dong, S. J. *J. Electroanal. Chem.* **1996**, *416*, 97.
(5) Zhao, Y.-D.; Pang, D.-W.; Hu, S.; Wang, Z.-L.; Cheng, J.-K.; Daib, H.-P. *Talanta* **1999**, *49*, 751.
(6) Molinero, V.; Calvo, E. J. *J. Electroanal. Chem.* **1998**, *445*, 17.
(7) Hobara, D.; Sasaki, T.; Imabayashi, S.; Kakiuchi, T. *Langmuir* **1999**, *15*, 5073.
(8) Murray, C. B.; Kagan, C. R.; Bawendi, M. G. *Annu. Rev. Mater. Sci.* **2000**, *30*, 545.
(9) Hutter, E.; Cha, S.; Liu, J. F.; Park, J.; Yi, J.; Fendler, J. H.; Roy, D. *J. Phys. Chem. B* **2001**, *105*.
(10) de Bruijin, H. E.; Altenburg, B. S. F.; Kooyman, R. P. H.; Greve, J. *Opt. Commun.* **1991**, *82*, 425.
(11) Roy, D. *Appl. Spectrosc.* **2001**, *55*, 1046.
(12) Kretschmann, E. *Z. Phys.* **1971**, *241*, 313.
(13) Raether, H. *Surface Plasmons on Smooth and Rough Surfaces and Gratings*; Springer-Verlag: New York, 1988.
(14) Hutter, E.; Fendler, J. H.; Roy, D. *J. Appl. Phys.* **2001**, *90*, 1977.

10.1021/la011226y CCC: $22.00
Published on Web 12/21/2001

and passes through a minimum at the SPR angle, θ_0^p. The SPR angle is extremely sensitive to structural and chemical (optical) properties of the SAM surface,[10−13] and it is this feature of the SPR technique that allows us to optically probe detailed surface modifications of the MPA layer. The carboxylic acid of the SAM in layer 3 can be protonated (below the pK_a) or deprotonated (above the pK_a) according to eq 1 by changing the pH of its adjacent medium 4:

$$\mathrm{RCOOH_{SAM}} \overset{\mathrm{p}K_a}{\rightleftharpoons} \mathrm{RCOO^-_{SAM}} + \mathrm{H^+_{SOLUTION}} \quad (1)$$

The pK_a of gold surface bound MPA was assessed to be about 7.7—a value of some 3.5 units higher than those found for similar acids in aqueous solution.[15−18] The increased pK_a was attributable to hydrogen bonding. Equation 1 is based on the model of SAM deprotonation where the dissociated H^+ is considered in the bulk solution.[15] We note here that some of the H^+ ions generated by SAM deprotonation may also reside in the double layer region. Here, we do not attempt to probe the detailed spatial distribution of the reaction product H^+ indicated in eq 1. Instead, we focus strictly on the detection of changes in the optical properties of the SAM layer as caused by protonation and deprotonation of this layer. It has been shown that below pH 6.0, MPA is fully protonated and above pH 10 it is fully ionized.[15] It is expected that (irrespective of the location of the H^+ generated in the forward reaction of eq 1) these changes of surface charges would affect both the electronic configuration and the orientation of the SAM layer. This would result in a change of the dielectric function ϵ_3 and, hence, the refractive index, $n_3 = (\epsilon_3)^{1/2}$, of the MPA SAM.[19] In this work, we probe these changes using SPR measurements. We start out with a SAM layer, characterized by the parameters ϵ_3 and d_3. For the ionized SAM, these parameters change to their respective new values, ϵ_3' and d_3'. These changes are manifested in a shift in the SPR angle, $\Delta\theta_0^p$. To correlate $\Delta\theta_0^p$ to changes in the dielectric function (refractive index), we assume that the number of MPA molecules in the SAM does not change by changes in ϵ_3 during the protonation/deprotonation of MPA. With this assumption, and using the Lorentz−Lorenz relation for refractive index of a two-component (water and MPA) system in the framework of Fresnel reflectivity equations, we obtain[19−21]

$$\Delta\theta_0^{\,p} \approx \Delta\epsilon_3\left[A - \frac{B(\epsilon_3 + 2)^{-1}}{(\epsilon_3 - 1) - f(\epsilon_3 + 2)}\right] \quad (2)$$

where $A = (A_o d_3)[1 + \{|\epsilon_{2r}|(\epsilon_3)^{-2}\epsilon_4\}]$, $B = (3\,A_0 d_3/\epsilon_3)[(|\epsilon_{3r}| + \epsilon_3)(\epsilon_3 - \epsilon_4)]$, ϵ_{2r} is the real part of ϵ_2, $\Delta\epsilon_3 = (\epsilon_3' - \epsilon_3)$, $\Delta d_3 = (d_3' - d_3)$, $f = [(\epsilon_4 - 1)/(\epsilon_4 + 2)](V_w/V)$, V_w is the volume occupied by water molecules in the SAM film, V is the total volume of this film, and

$$A_0 = \frac{2\pi(|\epsilon_{2r}|\epsilon_4)^{3/2}}{\lambda\epsilon_0^{\,1/2}\cos\theta_0^{\,p}(|\epsilon_{2r}| - \epsilon_4)^2(|\epsilon_{2r}| + \epsilon_4)} \quad (3)$$

During the ionization of the SAM, $\Delta\epsilon_3$ and, hence, $\Delta\theta_0^p$ should change and this change can be detected with high-resolution SPR measurements.[19,20] Earlier published SPR instruments allowed for a resolution of $\sim 2 \times 10^{-6}$ refractive index unit (RIU), corresponding to a sample thickness detection limit of 0.003 nm.[22] A recently reported method, based on bicell photodetection, allows for a resolution of $\sim 10^{-5}$ deg in the measurement of SPR angles (which corresponds to a detection limit for refractive index variations down to $\sim 10^{-8}$ RIU).[20,23] In the present work, we use the latter technique for time-resolved measurement of $\Delta\theta_0^p$. This method allows us to follow changes in ϵ_3 during the protonation or deprotonation of the MPA layer, as well as to monitor kinetics of SAM adsorption on a gold SPR substrate. Traditional SPR measurements, involving incidence angle dependence of the SPR reflectivity, are also employed here to estimate the characteristic parameters, ϵ_3 and d_3 of the protonated MPA. In this case, we fit experimental SPR ($R-\theta_0$) plots to a previously reported standard five-phase model of Fresnel reflectivity[9−11] with known d_1, d_2, ϵ_1, ϵ_2, and ϵ_4, and trial values d_3, and ϵ_3. Subsequently, the resulting values of ϵ_3 can be plotted against those of d_3 for two different choices of ϵ_4. The unknown d_3 and ϵ_3 can be determined from these plots by using previously reported methods[10,24−26] that employ two different solvents (water and ethanol, in the present work) and two different lasers for excitation (632.8 and 850.0 nm, in the present case). When the term V_w/V is known (or can be estimated), one can estimate $\Delta\epsilon_3$ from the experimentally measured $\Delta\theta_0^p$ by using the initial parameters, ϵ_3 and d_3, of the SAM in eq 2. Estimates for $\Delta\epsilon_3$ and Δn_3 based on these considerations are presented later in this report.

3. Experimental Section

MPA ($SHCH_2CH_2COOH$, Aldrich), sulfuric acid, hydrochloric acid (Fischer), sodium hydroxide (Aldrich), ethanol (anhydrous, Pharmco), and 30% hydrogen peroxide (Fisher) were used as received. Water was purified by a Milli-QTM Millipore system. Preparation of the Au SPR substrates is described in our earlier work.[9,14] In brief, Au films were deposited in a vacuum chamber (Edwards, AUTO 306) using Cr binder layers on clean microscope slides (Fisher Scientific, finest Premium, SF10, 3 in. × 1 in.). The thicknesses of the Cr and Au films were monitored using a quartz crystal microbalance (QCMB). Just prior to self-assembly the substrates were cleaned by immersion into piranha solution and copiously rinsed by water and ethanol. A set of preliminary experiments were performed to separate the role of the ambient solution in the pH-dependent SPR response of the experimental system. We found that changing buffer solutions affected the SPR data (by affecting the refractive index of medium 4), irrespective of the presence of the SAM layer 3 in the multilayer structure. Therefore, instead of using buffer solutions, we used HCl and NaOH to control the pH of the ambient medium. No intrinsic optical effects of these latter solutions were detected. Immersion of the cleaned substrate into a 1.0 mM aqueous MPA solution (pH = 3.0 adjusted by HCl), for 10 min resulted in the self-assembly, a monolayer of MPA on the Au substrate. The instrument used for angle-resolved SPR measurements is described elsewhere.[9] In brief, the sample was optically coupled

(15) Hu, K.; Bard, A. J. *Langmuir* **1997**, *13*, 5114.
(16) Kane, V.; Mulvaney, P. *Langmuir* **1998**, *14*, 3303.
(17) Godínez, L. A.; Castro, R.; Kaifer, A. E. *Langmuir* **1996**, *12*, 5087−5092.
(18) Kakiuchi, T.; Iida, M.; Imabayashi, S.; Niki, K. *Langmuir* **2000**, *16*, 5397−5401.
(19) Salamon, Z.; Macleod, H. A.; Tollin, G. *Biochim. Biophys. Acta* **1997**, *1331*, 117.
(20) Boussaad, S.; Pean, J.; Tao, N. J. *Anal. Chem.* **2000**, *72*, 222.
(21) Roy, D. Unpublished results, 2001.
(22) Jung, L. S.; Campbell, C. T.; Chinowsky, T. M.; Mar, M. N.; Yee, S. S. *Langmuir* **1998**, *14*, 5636.
(23) Tao, N. J.; Boussaad, S.; Huang, W. L.; Arechabaleta, R. A.; D'Agnese, J. *Rev. Sci. Instrum.* **1999**, *70*, 4656.
(24) Peterlinz, K. A.; Georgiadis, R. *Opt. Commun.* **1996**, *130*, 260.
(25) Peterlinz, K. A.; Georgiadis, R. M.; Herne, T. M.; Tarlov, M. J. *J. Am. Chem. Soc.* **1997**, *119*, 3401.
(26) Peterlinz, K. A.; Georgiadis, R. *Opt. Commun.* **1996**, *130*, 260. Nelson, B. P.; Frutos, A. G.; Brockman, J. M.; Corn, R. M. *Anal. Chem.* **1999**, *71*, 3928. Frutos, A. G.; Weibel, S. C.; Corn, R. M. *Anal. Chem.* **1999**, *71*, 3935.

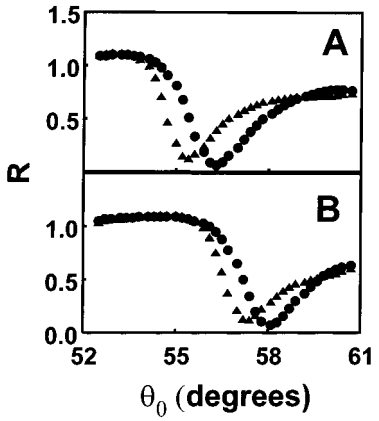

Figure 1. Incident angle (θ_0) dependent SPR reflectivity (R) for four-phase (triangles) and five-phase (circles) multilayer systems, using ambient dielectrics of water (pH = 3, panel A) and ethanol (panel B). For each graph, every fourth point from the collected raw data is plotted to preserve clarity of the plot. The four-phase system corresponds to a SAM-free Au SPP substrate. In the five-phase case, the Au substrate is coated with a SAM of MPA by immersing the Au in 1.0 mM aqueous (in A) or ethanolic solution (in B) of MPA.

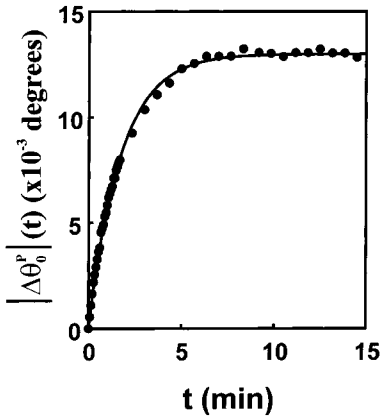

Figure 2. Kinetic behavior of SAM formation of MPA on Au in an aqueous acidic solution (pH = 3.0, adjusted with HCl) of 1.0 mM MPA. The symbols represent the magnitude of the SPR angle shifts. Every fourth point from the raw data is plotted here to preserve clarity of the plot. The line through the symbols represents the fit of eq 4 to the experimental data.

to a prism (SF 10) using a refractive index matching fluid (R.P. Cargille Laboratories). The sample was immersed in deionized water contained in a Teflon cell. Two different lasers were used (a 2 mW He−Ne, 632.8 nm and a 2 mW diode laser, 850 nm) in conjunction with a large area silicon detector (Newport, 818-SL) for the angle-scan SPR measurements. The thicknesses and the dielectric constant (at a given pH) of the MPA SAM were estimated by using a combined two-solvents, two-color method, described by previous authors.[24−26] The time-resolved SPR measurements were performed using the 635 nm incident wavelength (using a 5 mW diode Power Technologies laser) and a bicell photodiode detector (Hamamatsu), following the previously described procedure.[20,23] The photocurrents, from the two photocells, were converted to voltages, and collected on a computer. This method provides an accurate, time-resolved detection with high angular resolution ($\sim 10^{-3}-10^{-4}$ deg for our instrument) and fast time response (~ 1 μs).[23] In situ SAM ionization and reprotonation experiments were performed by changing the aqueous solution bathing the MPA SAM to the desired pH, adjusted by HCl or NaOH. All experiments reported here are performed at room temperature.

4. Results and Discussion

Angle-dependent SPR plots using an ambient dielectric of water (pH = 3) are presented in Figure 1A. For comparison with this case, another set of SPR plots are shown in Figure 1B where a different ambient dielectric, ethanol, is used. In each panel of Figure 1, the triangles and the circles correspond to the four-phase (0124, the gold substrate without the SAM) and five-phase (01234, the gold substrate with completely formed MPA SAM) systems, respectively. The SPR angles (positions of reflectivity minima) for the (0124) structures are different in panels A (55.4°) and B (57.3°), because these angles depend on ϵ_4, which in turn is different for water and ethanol. The adsorption of the SAM layer shifts the SPR angle, and because this shift also depends on ϵ_4, the SPR angles for the five phase (01234) structures are different for water (56.5° in A) and ethanol (58.1° in B). The SPR system corresponding to the data shown with the circles in Figure 1A represents the initial fully protonated MPA.

For in situ SPR measurements of SAM ionization, it is necessary to induce deprotonation in the same experimental cell where the SAM is formed on Au. This requires a knowledge of the SAM formation time, because the pH of the ambient dielectric must be changed only after the complete SAM is formed. When a SAM is being formed on the Au substrate, the SPR angle would shift according to eq 2, and eventually, would stop changing when saturation surface coverage of the SAM is achieved.[24,25] From considerations similar to those of eqs 2 and 3, it can be shown that changes in the surface coverage of a SAM are also proportional to the angular shifts, $\Delta\theta_0^{\rm p}(t)$, that occur during the formation of the SAM.[21,25] Thus, the time-resolved SPR technique mentioned in section 2 can be employed to determine the SAM adsorption saturation time. In Figure 2, we present sample results of SPR experiments based on these considerations. Here, the Au SPR substrate is introduced in 1 mM aqueous solution (pH = 3.0) of MPA, and $\Delta\theta_0^{\rm p}(t)$ is measured as a function of time. The symbols represent experimental data. As seen here, the SAM formation is complete within ~10 min after exposing the Au substrate to the MPA solution. We also find that $\Delta\theta_0^{\rm p}$ in Figure 2 follows a first-order Langmuir adsorption kinetic

$$\mathrm{d}(\Delta\theta_0^{\rm p})/\mathrm{d}t = k_{\rm a}[1 - (\Delta\theta_0^{\rm p}/\Delta\theta_{0\rm s}^{\rm p})] \qquad (4)$$

where $\Delta\theta_0^{\rm p}(t{=}0) = 0$, $\Delta\theta_{0\rm s}^{\rm p}$ is the final value of $\Delta\theta_0^{\rm p}$ corresponding to saturation of SAM adsorption, and $k_{\rm a}$ is the rate constant of SAM formation on Au. The line in Figure 2 shows the fit of eq 4 to the experimental data, and $k_{\rm a}$ is determined to be 7.54×10^{-3} min^{-1} from this fit.

As mentioned earlier, the fully formed MPA SAM on Au can be characterized by the parameters ϵ_3 and d_3. Although the main focus of our present experiments is to probe relative changes in these parameters, it is possible to utilize two-solvent experiments such as those of Figure 1 to estimate ϵ_3 and d_3 for the complete MPA SAM. Such an estimate is based on the assumption that d_3 for MPA does not vary considerably by changing the ambient liquid from water to ethanol.[27] Within the limits of this assumption, and following the procedure for the two-solvent technique outlined by previous authors,[24,25] we estimate $\epsilon_3 \approx 2.12$, and $d_3 \approx 0.50$ nm. These values were substantiated by the two-color determination [26]of ϵ_3 and d_3. The combined two-solvent and two-color plots provide a value of $d_3 = 0.50 \pm 0.02$ nm (Figure 3). In the calculation of these parameters, we also use the following measured and known quantities: $d_1 = 0.4$ nm, $d_2 = 42.8$ nm (d_1 and

(27) Schlenoff, J. B.; Li, M.; Ly, H. *J. Am. Chem. Soc.* **1995,** *117,* 12528.

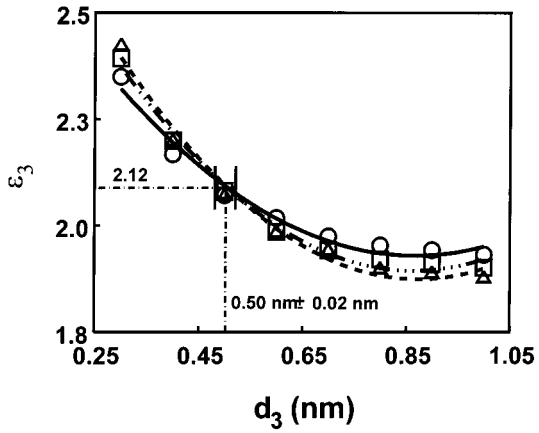

Figure 3. Determination of the thickness (d_3) and the dielectric function (ϵ_3) of a SAM of MPA (layer 3) in a five-phase (01234) multilayer, with pH 3 water (data points shown by triangles, dashed line) and ethanol (data points shown by circles, solid line) by using a 632.8 nm laser and in pH 3 water by using a 850.0 nm laser (data points shown by squares, dash-dotted line). The symbols correspond to trial values of d_3 and ϵ_3 that are used to fit a five-phase model of Fresnel reflectivity to experimental SPR plots such as those shown with the circles in Figure 1. The lines represent empirical polynomial fits to the parameters indicated by the symbols. The point of intersection ($d_3 = 0.50 \pm 0.02$ nm, $\epsilon_3 = 2.12$) of the three lines represents the values of d_3 and ϵ_3 for the MPA SAM. The range of uncertainty (error bar) in the value of d_3 is indicated by the two vertical lines next to the point of intersection of the three plots.

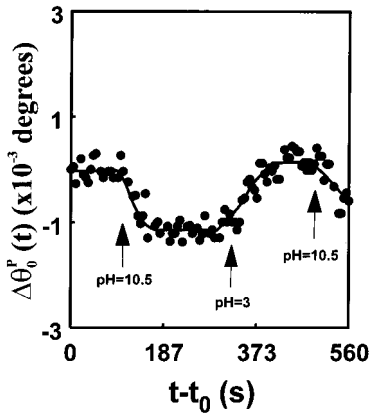

Figure 4. Effects of changing solution pH (in medium 4) on the SPR angle for a five-phase multilayer structure including a completely formed SAM of MPA. The MPA SAM is formed in an aqueous solution of 1 mM MPA at pH 3 (as in Figure 2), and allowed to stabilize for a relatively long time, t_0 (~55 min). At $t > t_0$, the solution pH is repeatedly changed between 3 and 10.5. The symbols represent experimental data, and the arrows indicate the points in time when HCl (at $t - t_0 = 335$ s) or NaOH (at $t - t_0 = 115$ and 495 s) is introduced in the cell to change the solution pH. The line through the symbols shows the general trend of variations exhibited by the data.

d_2 are determined with the QCMB instrument mentioned in the Experimental Section); for $\lambda = 632.8$ nm, $\epsilon_1 = -5.60 + i(31.95)$,[28] $\epsilon_2 = -11.8625 + i(0.2206)$,[9,13] $\epsilon_4 = 1.7769$ (water),[29] and $\epsilon_4 = 1.8469$ (ethanol),[29] where $i = (-1)^{1/2}$; for $\lambda = 850.0$ nm, $\epsilon_1 = -31.12 + i(30.35)$, $\epsilon_2 = -22.9525 + i(0.2206)$,[13] and $\epsilon_4 = 1.7769$ (water). From a computer simulation (using the Chempen3D (Hilton) software without optimizing the geometry), we calculated the length of the MPA molecule to be 0.773 nm. The above estimated value of d_3 in Figure 3 corresponds to a ~ 40.4° tilt angle of such a molecule in its adsorbed state on the Au surface. Next, we proceed to examine the pH-dependent ionization behavior of a completely formed MPA SAM using time-resolved SPR measurements. We introduce the Au substrate in 1.0 mM aqueous solution (pH = 3) of MPA and monitor the $\Delta\theta_0^p(t)$ behavior of this system (as done in Figure 2). Sufficient time after the SAM is formed and stabilized (and $\Delta\theta_0^p$ is settled at its time-independent value), at a time t_0, we change the pH of the solution to 10.5. Following subsequent stabilization of the SPR angle, again we change back the pH of the solution to 3. The results for two such cycles of pH alterations are presented in Figure 4. Here, $t_0 \approx 55$ min, and the arrows indicate the instants when the solution pH is changed by injection of HCl or NaOH into the experimental cell. A definite trend of variations, above the experimental noise level and following the sequence of pH changes, is observed in the $\Delta\theta_0^p(t)$ data (symbols) of Figure 4. The line through the data represents this trend to guide the eye. We find that the variations of $\Delta\theta_0^p(t)$ seen in Figure 4 are not observed when we repeat the pH-dependent SPR measurements of Figure 4 using a SAM-free Au substrate and keeping all other experimental conditions unchanged. Therefore, we attribute the observed pH-dependent changes of the SPR angles in Figure 4 to morphological changes of the MPA SAM caused by ionization and reprotonation of the SAM. The SPR angle increases when MPA is protonated in the acid environment, and the reverse situation is observed in base solution. Furthermore, the changes of the SPR angles are reversible with respect to the ionization and reprotonation, as well as with respect to repetitive cycling of pH alterations. The change in the SAM dielectric function indicated by the observed SPR angle shifts can be estimated from eq 2 using sample values (0.0 and 0.5) of the term, V_w/V. In Figure 4, the SPR angle shifts by $\sim -0.001°$ (-1.74×10^{-5} radians) due to a change in the solution pH from 3.0 to 10.5. According to eq 2, this corresponds to $\Delta\epsilon_3 \approx -1.08 \times 10^{-2}$ for $V_w/V = 0$ (compact SAM), and $\Delta\epsilon_3 \approx -1.37 \times 10^{-2}$ for $V_w/V = 0.5$ (loosely packed SAM). Cyclic voltammograms of the $[Fe(CN)_6]^{3-}/[Fe(CN)_6]^{4-}$ redox couple in aqueous 0.1 M KCl solutions indicated only a modest decrease of the current on forming the MPA SAM.[30] Therefore, considering the relatively short length and pinhole-containing nature of MPA SAMs, the latter one of the two above estimated values for $\Delta\epsilon_3$ is likely to be more realistic. In terms of changes in the refractive index ($\Delta n_3 = \Delta\epsilon_3/2n_3$) of the MPA layer, the above-mentioned values correspond to Δn_3 ($V_w/V = 0$) $\approx -3.73 \times 10^{-3}$ RIU, and Δn_3 ($V_w/V = 0.5$) $\approx -4.73 \times 10^{-3}$ RIU. Accurate measurement of these parameters will require further experiments that would focus, in particular, on careful determination of the SAM packing density.[31,32] Nevertheless the above-estimated values provide an over all description of the optical response of the MPA surface to the ionization−reprotonation reactions.

5. Conclusions

Demonstrating the sensitivity of SPR measurements to monitor the rate of self-assembly of a layer of MPA and

(28) Bos, L. W.; Lynch, D. W. *Phys. Rev. B* **1970**, *2*, 4567.
(29) *Handbook of Chemistry and Physics*, 64th ed.; CRC Press: Boca Raton, FL, 1983−1984; p E368.
(30) Fendler, J. H. Unpublished results, 2001.
(31) Brockman, J. M.; Nelson, B. P.; Corn, R. M. *Annu. Rev. Phys. Chem.* **2000**, *51*, 41.
(32) Yang, D.; Zi, M.; Chen, B.; Gao, Z. *J. Electroanal. Chem.* **1999**, *470*, 114.

that of its ionization and reprotonation are the main accomplishments of the present report. Obtaining an increasingly deeper insight into interactions at organized nanostructures continues to be the subject of our intense scrutiny.

Acknowledgment. This work was funded in part by the National Science Foundation and by the BK21 Program of the Korean Ministry of Education.

LA011226Y